Supplementary Information

Exciting Hybrid Optical Modes with Fano Lineshapes in Core-Shell $CsPbBr_3$ Microspheres for Optical Sensing

Xin Zhao,[1] Shulei Li,[1,2] Weichen He, [1] Maohui Yuan,[1] Jingdong Chen[3*] and Sheng Lan[1*]

1. Guangdong Provincial Key Laboratory of Nanophotonic Functional Materials and Devices, School of Information and Optoelectronic Science and Engineering, South China Normal University, Guangzhou 510006, China

2. School of Optoelectronic Engineering, Guangdong Polytechnic Normal University, Guangzhou 510665, P. R. China

3. College of Physics and Information Engineering,
Minnan Normal University, Zhangzhou 363000, China

*Corresponding author: jdchen@163.com and slan@scnu.edu.cn

Supplementary Note S1: Scattering spectra of PS microspheres with different diameters placed on SiO_2 and Au/SiO_2 substrates

We examined the scattering spectra of PS microspheres with different diameters placed on SiO_2 and Au/SiO_2 substrates by using numerical simulations based on the FDTD technique. The PS microspheres were excited by *p*- and *s*-polarized light in a total internal reflection configuration. The calculated scattering spectra are presented in Figure S1. It was found that the quality factors of the optical modes increase with increasing diameter of the PS microsphere. In addition, it was noticed that sharp optical modes with large quality factors can be achieved for the PS microsphere with D = 4.3 μm placed on the Au/SiO_2 substrate and excited with *s*-polarized light, as shown in Figure S1d. The calculated results are in good agreement with the measured ones (see Figure 1).

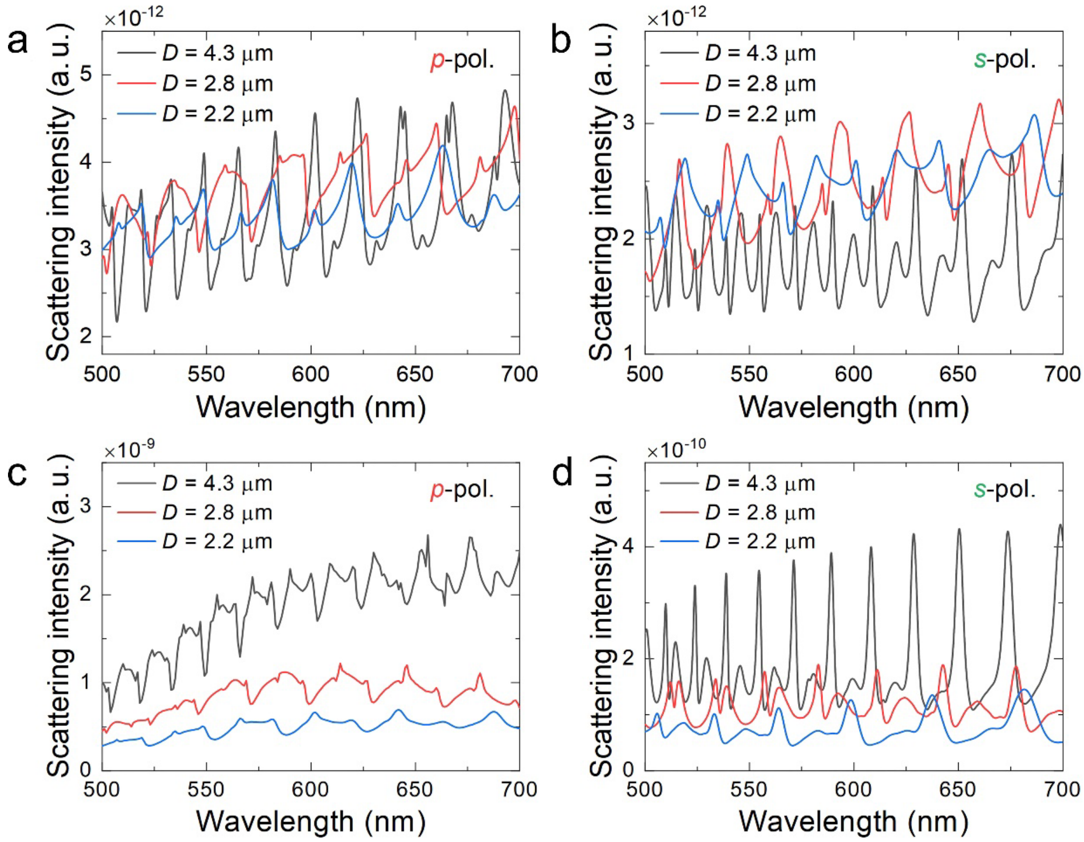

Figure S1. Scattering spectra simulated of PS microspheres with different diameters placed on a SiO_2 substrate and excited by using the evanescent wave generated with (a) *p*- and (b) *s*-polarized light. The scattering spectra simulated of PS microspheres with the same diameters placed on an Au/SiO_2 substrate and excited by using the evanescent wave generated with *p*- and *s*-polarized light are shown in (c) and (d).

Supplementary Note S2: Electric field distributions in the PS microsphere with D = 4.3 μm placed on the SiO_2 substrate

We calculated the scattering spectrum of the PS microsphere with D = 4.3 μm placed on the SiO_2 substrate and excited by using the evanescent wave generated with *s*-polarized light, as shown in Figure S2a. The electric field ($|E_y/E_0|$) and ($|E/E_0|$) distributions at three wavelengths (λ = 539, 541 and 546 nm) corresponding to the scattering peaks and scattering dip are shown in Figure S2b.

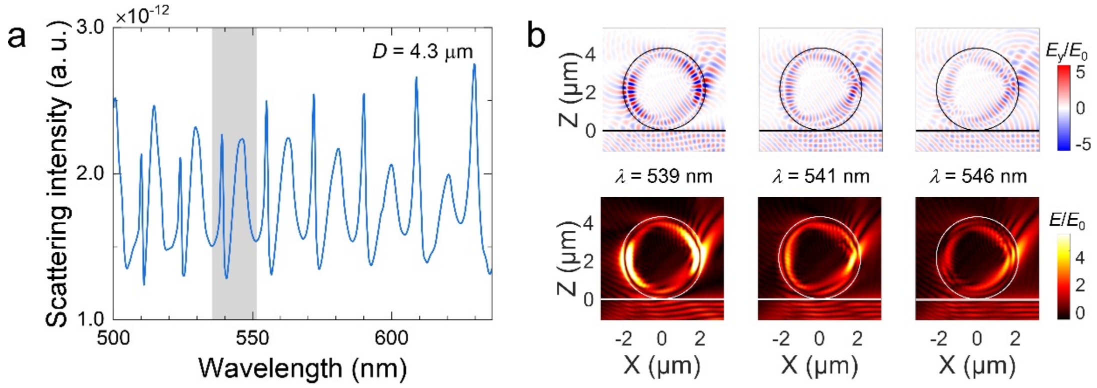

Figure S2. (a) Scattering spectra simulated of a PS microsphere with D = 4.3 μm placed on an SiO_2 substrate excited by using the evanescent wave generated with *s*-polarized light. (b) Electric field ($|E_y/E_0|$) and ($|E/E_0|$) distributions calculated for the hybrid optical modes supported by a PS microsphere with D = 4.3 μm.

Supplementary Note S3: Element distributions in $CsPbBr_3$ microspheres

We examined the element distributions in $CsPbBr_3$ microspheres by using energy dispersion spectroscopy (EDS) analysis. A typical example is shown in Figure S3 in which we can see the uniform spatial distributions of Cs, Pb and Br in the $CsPbBr_3$ microsphere.

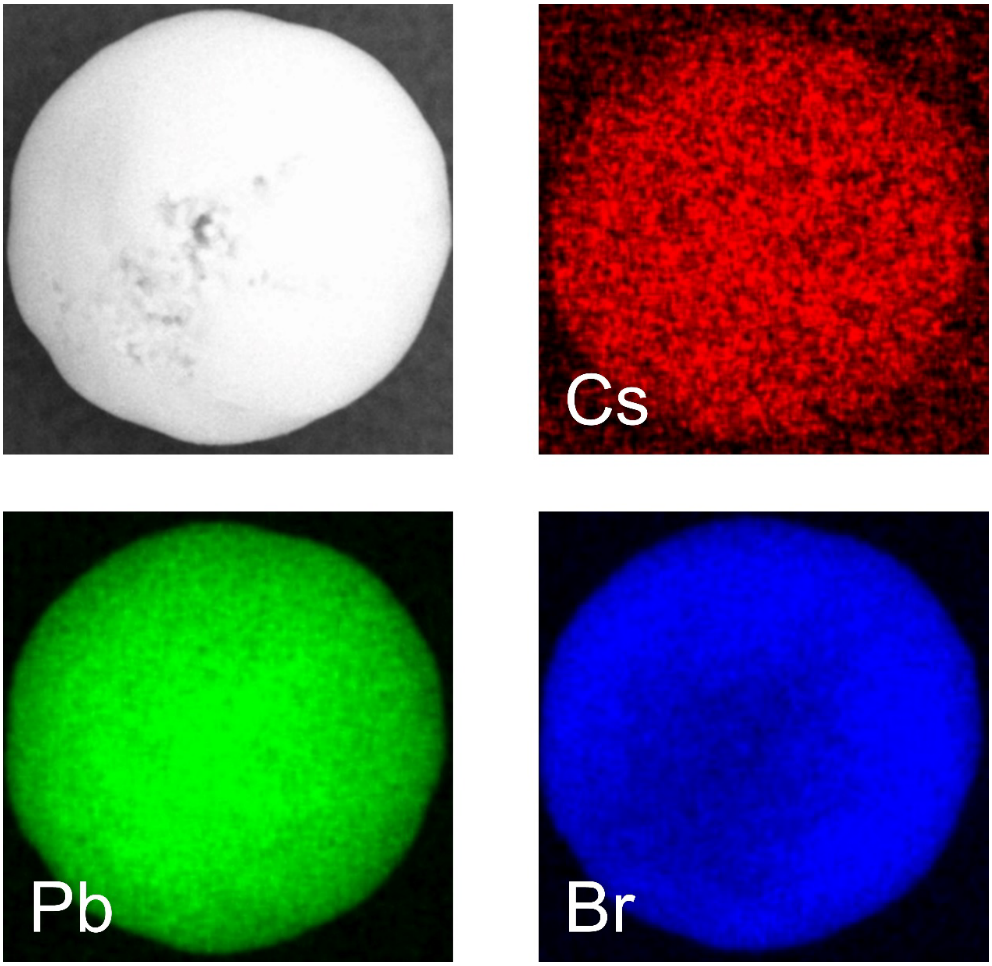

Figure S3. The energy dispersive spectroscopy (EDS) mapping carried out for a typical $CsPbBr_3$ microsphere, which indicates the uniform spatial distribution of the constituent elements (i.e., Cs, Pb, and Br).

Supplementary Note S4: Crystalline structures of $CsPbBr_3$ microspheres before and after the phase transition and element distributions in $CsPbBr_3$ microspheres

We characterized the crystalline structures of $CsPbBr_3$ microspheres by using transmission electron microscopy (TEM). A typical example is shown in Figure S4a where the evolutions of the TEM image and electron diffraction pattern of a $CsPbBr_3$ with a diameter of D ~ 1.6 μm upon the irradiation of electron beam observed are presented. It can be seen that the surface structure of the microsphere is different from the inner structure at the initial stage (t = 1.0 s, upper panel). In addition, a Debby–Sherrer ring is observed in the electron diffraction pattern, implying that the surface structure is polycrystalline in this case. After irradiated by electron beam for some time (t = 10.0 s, lower panel), one can see distinct Bragg diffraction spots in the electron diffraction pattern. Moreover, the difference between the surface structure and the inner structure disappears in the TEM image. Therefore, we think that the $CsPbBr_3$ possesses a core-shell structure. To further confirm this suspect, we performed X-ray photoelectron spectroscopy (XPS) measurements for $CsPbBr_3$ microspheres and a typical example is shown in Figure S4b. In this case, the $CsPbBr_3$ microsphere was etched by using Ar ions while the elements on the surface of the microsphere were measured. It is noticed that the element ratios of Cs, Pb, and Br were 5.03%, 15.09%, 79.88% at the initial stage. After etching of t = 5.0 min, the element ratios became 5.29%, 28.27%, 66.44%. It also indicates that the inner structure is different from the surface structure, supporting the core-shell structure of the $CsPbBr_3$ microsphere.

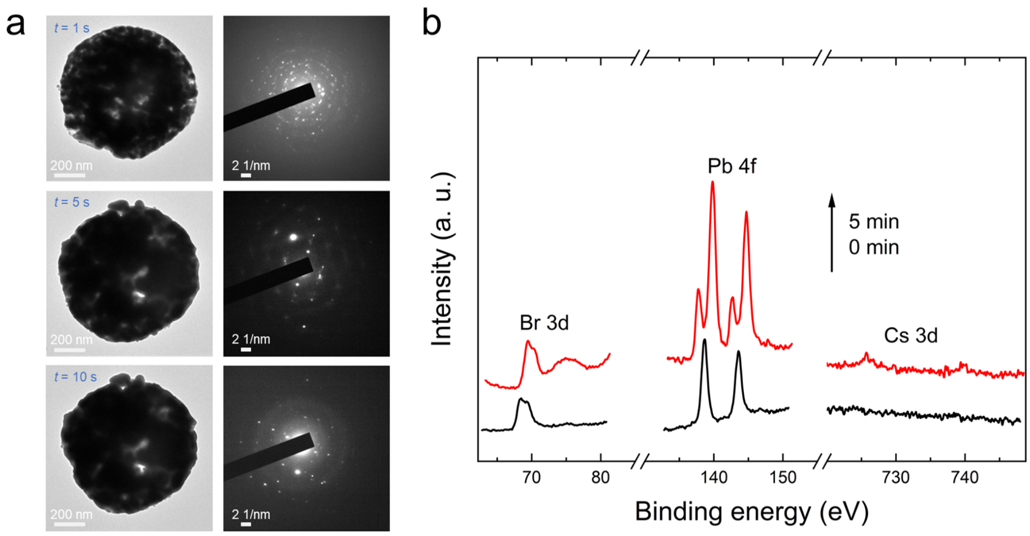

Figure S4. (a) Evolution of the TEM image and electron diffraction pattern of a $CsPbBr_3$ microsphere (D ~ 1.6 μm) induced by the irradiation of electron beam during the TEM measurements. (b) XPS spectra observed for a $CsPbBr_3$ microsphere at different etching times.

Supplementary Note S5: Scattering spectra of $CsPbBr_3$ microspheres excited by *p*- and *s*-polarized light

We measured the scattering spectra of a $CsPbBr_3$ microsphere with D = 1.6 μm on the SiO_2 substrate, which was excited by using *p*- and *s*-polarized light. The results are shown in Figure S5. It can be seen that the optical modes generated by using *s*-polarized light possess larger Q factors than those generated by using *p*-polarized light. However, the Q factors of the optical modes obtained by using *s*-polarized light are smaller than those observed for $CsPbBr_3$ placed on the Au/SiO_2 substrate.

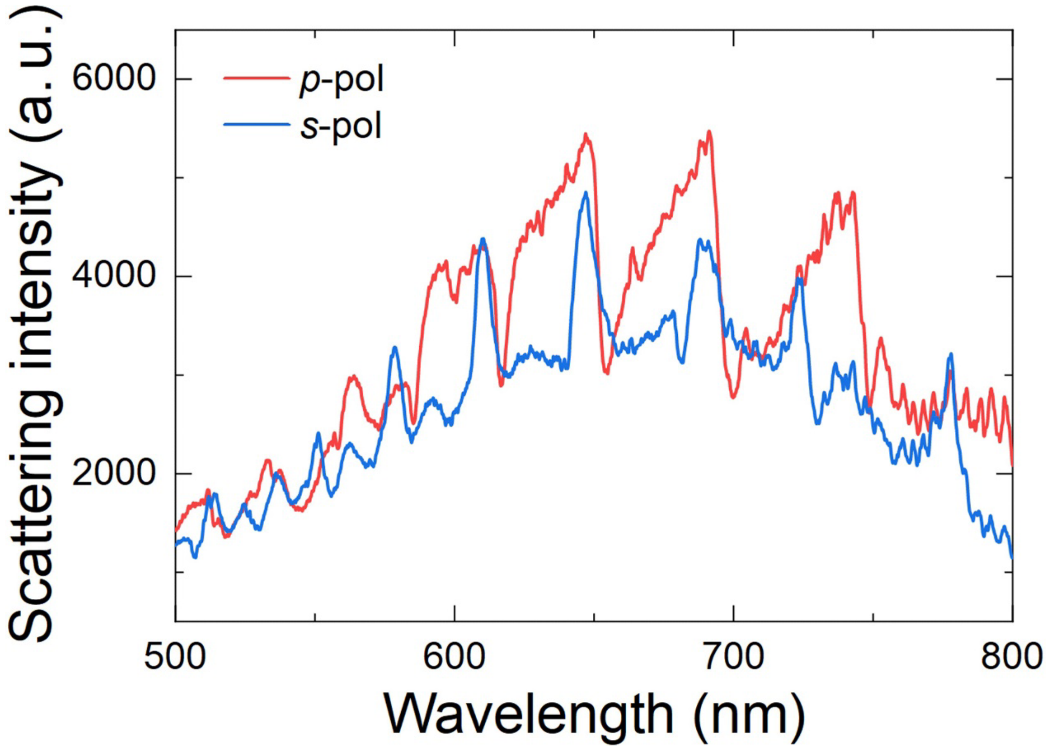

Figure S5. Scattering spectra of a $CsPbBr_3$ microsphere on a SiO_2 substrate excited by using *p*- and *s*-polarized light.

Supplementary Note S6: The refractive indices of $CsPbBr_3$, CsBr, and $PbBr_2$ used in the numerical simulations

We established a core-shell model for $CsPbBr_3$ microspheres and the refractive indices of $CsPbBr_3$, CsBr, and $PbBr_2$ were taken from literatures (see Refs. 38-40). Since the shell was composed of CsBr and $PbBr_2$, the refractive index of the shell was taken as the averaged value of these two materials. The refractive indices of $CsPbBr_3$, CsBr and $PbBr_2$ taken from the literatures (see Refs. 38-40) are presented in Figure S6.

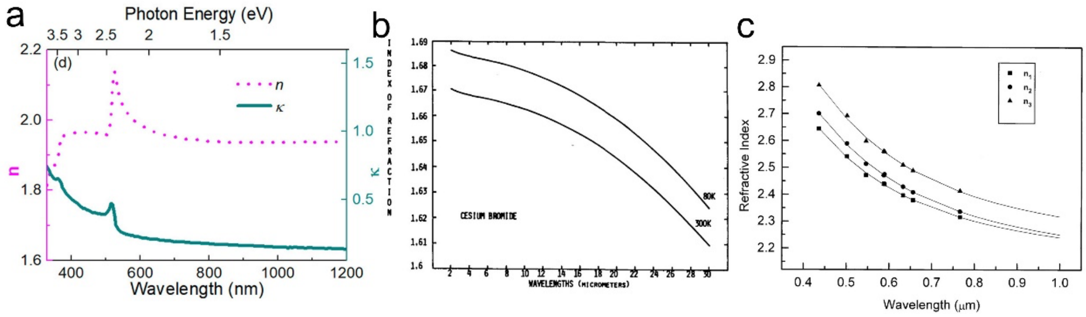

Figure S6. (a) The refractive index of the $CsPbBr_3$ crystal in the spectral range from near-ultraviolet to near-infrared (from Ref. 38). (b) The measured refractive indices as a function of wavelength of CsBr crystal (from Ref. 39). (c) The refractive index dispersion of the $PbBr_2$ crystal in the spectral range 420-1000 nm (from Ref. 40).

Supplementary Note S7: Scattering spectra of $CsPbBr_3$ microspheres placed on an Au/SiO_2 substrate

We measured the scattering spectra of a $CsPbBr_3$ on the Au/SiO_2 substrate, which was excited by using *s*-polarized at different incident angles, as shown in Figure S7. It was found that the resonant wavelengths of the optical modes excited in the microsphere do not change with the incident angle. However, the intensities of these optical resonances exhibit a dependence on the incident angle.

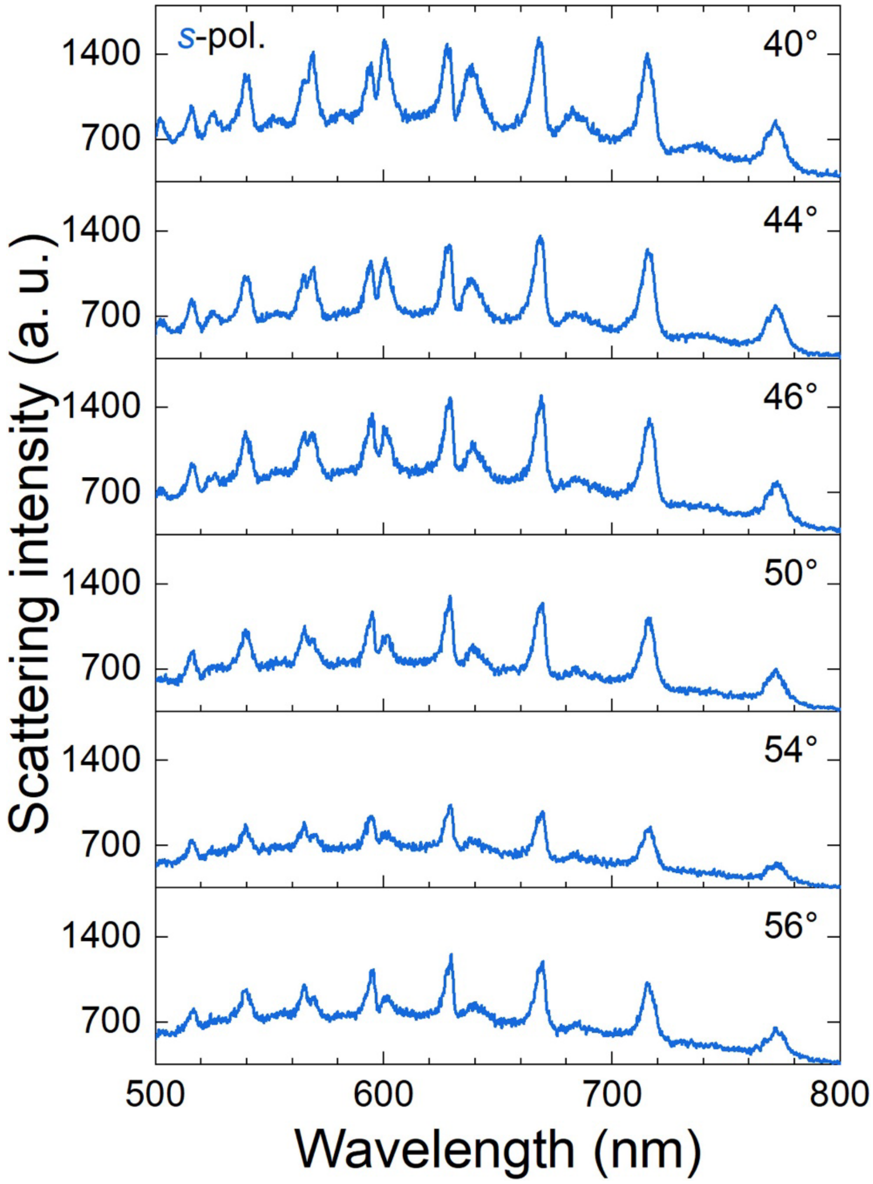

Figure S7. Scattering spectra measured for a $CsPbBr_3$ microsphere on the Au/SiO_2 substrate excited by using *s*-polarized light with different incident angles.

Supplementary Note S8: Electric field distributions in $CSPbBr_3$ microspheres with *D* = 1.5 μm and *d* = 700 nm placed on the Au/SiO_2 substrate

We simulated the scattering spectrum of a $CsPbBr_3$ microsphere with *D* = 1.5 μm and *d* = 700 nm placed on an Au/SiO_2 substrate and excited with *s*-polarized light, as shown in Figure S8a. In addition, we calculated the electric field amplitude/intensity distributions at three different wavelengths, which correspond to the scattering peaks and scattering dip in the scattering spectrum, as shown in Figure S8b. It is noticed that the electric field distribution at λ = 570 nm is very close to that of a WGM, verifying the physical origin of the hybrid optical modes.

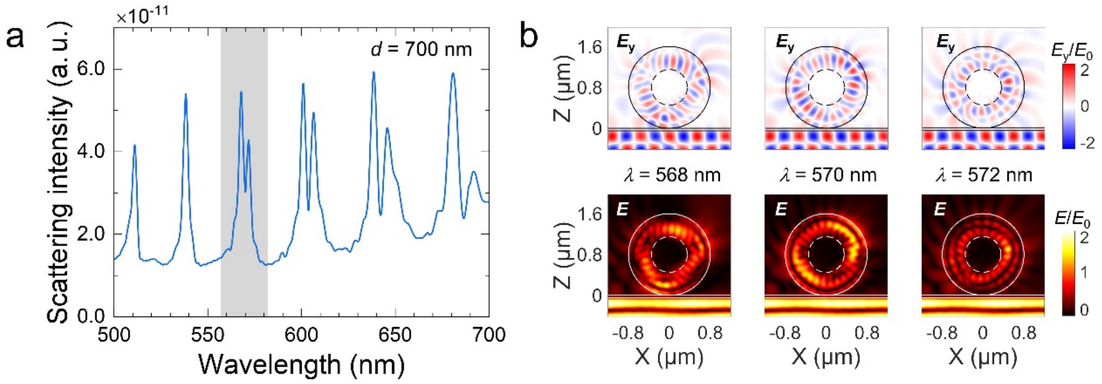

Figure S8. (a) Scattering spectra simulated for a core-shell $CsPbBr_3$ microsphere with *D* = 1.5 μm and *d* = 700 nm placed on an Au/SiO_2 substrate and excited with *s*-polarized light. (b) Electric field ($|E_y/E_0|$) and ($|E/E_0|$) distributions calculated for the hybrid optical modes supported by the core-shell $CsPbBr_3$ microsphere.

Supplementary Note S9: Scattering spectra of PS and $CsPbBr_3$ microspheres calculated by using Mie theory

We calculated the scattering spectra of a PS microsphere and a $CsPbBr_3$ with the same diameter of D = 1.6 μm by using the Mie theory, as shown in Figure S9. In each case, the scattering spectrum has been decomposed into the contributions of electric and magnetic multipoles with different orders. It can be seen that the scattering spectrum of the PS or the $CsPbBr_3$ microsphere in the visible light is dominated by the high-order Mie resonances.

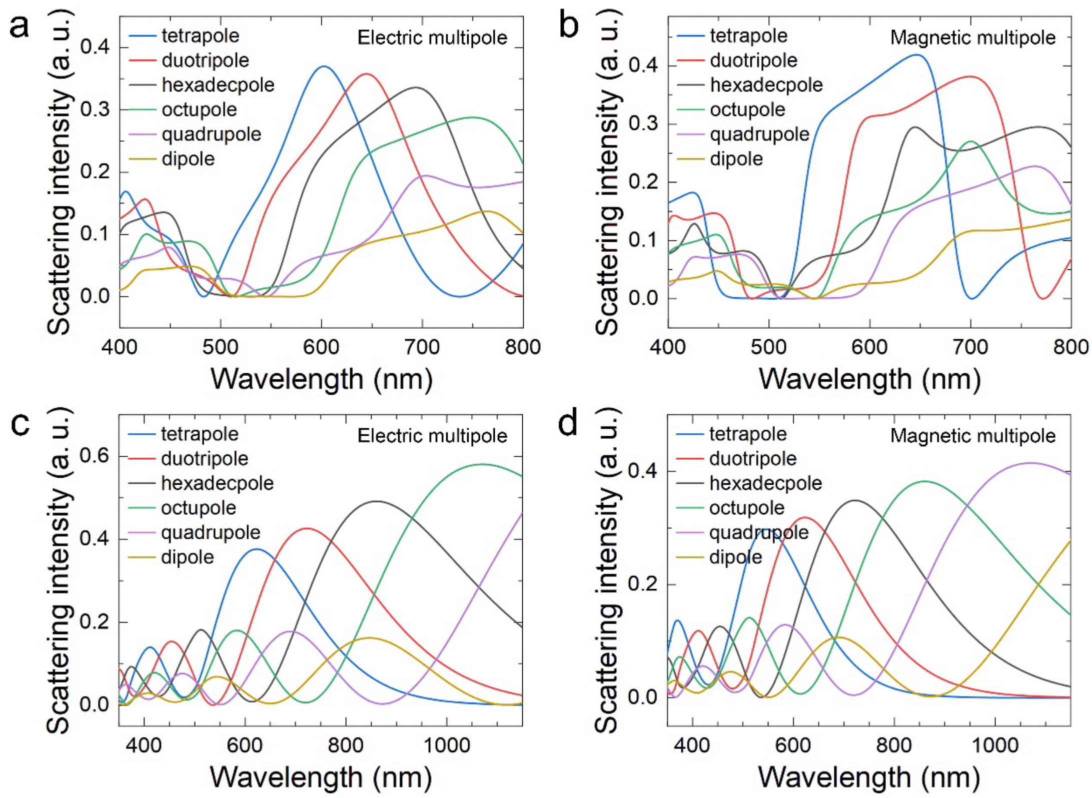

Figure S9. Electric (a) and magnetic (b) multipole scattering spectra calculated for a PS microsphere with D = 1.6 μm based on the Mie theory. The electric and magnetic multipole scattering spectra calculated for a $CsPbBr_3$ microsphere with D = 1.6 μm are shown in (c) and (d), respectively.

Supplementary Note S10: Sensing of environment humidity

In order to quantitatively characterize the sensitivity of the hybrid optical modes to the environment humidity, we measured the scattering spectra of a $CsPbBr_3$ under different humidity environments with the experimental setup shown in Figure S10a. The dependence of the peak position of an optical mode at 678 nm (as indicated by the arrow) on the environment humidity extracted from the evolution of the scattering spectrum is shown in Figure S10b. A blueshift of the optical mode was observed with increasing humidity and it exhibits a linear relationship when the humidity is smaller than 83%. For humidity larger than 83%, a rapid blueshift was observed.

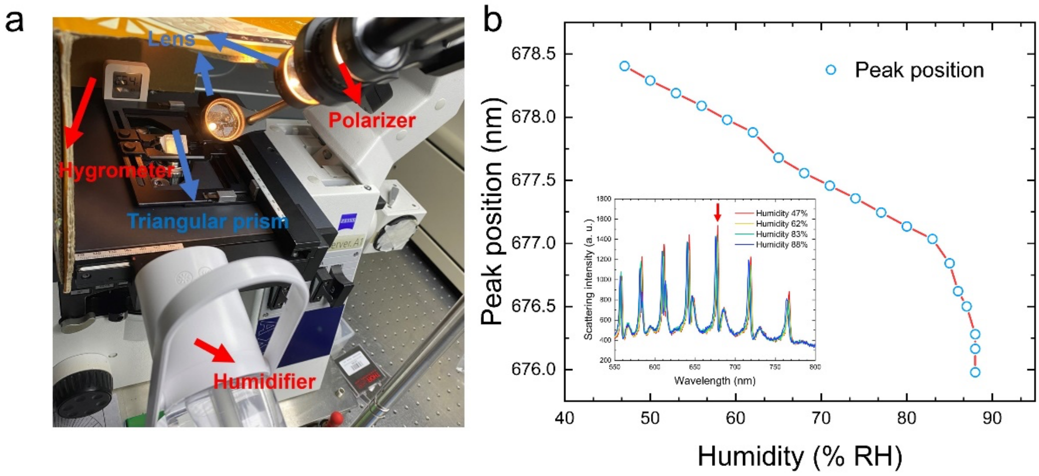

Figure S10. (a) Experimental setup used to measure the scattering spectra of a $CsPbBr_3$ microsphere under different humidity environments. (b) Dependence of the peak position of an optical mode of a $CsPbBr_3$ microsphere at 678 nm (as indicated by the arrow) on the environment humidity extracted from the scattering spectra of the microsphere under different humidity environments. The evolution of the scattering spectrum of the $CsPbBr_3$ microsphere with increasing environment humidity is shown in the inset.